The American Journal of Pathology, Vol. 170, No. 1, January 2007

DOI: 10.2353/ajpath.2007.060158

Epithelial and Mesenchymal Cell Biology

αvβ6 Integrin Regulates Renal Fibrosis and Inflammation in Alport Mouse

Kyungmin Hahm,* Matvey E. Lukashev,* Yi Luo,* William J. Yang,* Brian M. Dolinski,* Paul H. Weinreb,* Kenneth J. Simon,* Li Chun Wang,* Diane R. Leone,* Roy R. Lobb,* Donald J. McCrann,* Normand E. Allaire,* Gerald S. Horan,* Agnes Fogo,† Raghu Kalluri,‡§¶ Charles F. Shield III,‖ Dean Sheppard,** Humphrey A. Gardner,* and Shelia M. Violette*

From the Departments of Exploratory Biology, Fibrosis, Protein Chemistry, Gene Discovery, Molecular Profiling, and Research Pathology, Biogen Idec, Cambridge, Massachusetts; the Department of Pathology,† Vanderbilt University School of Medicine, Nashville, Tennessee; the Center for Matrix Biology,‡ Department of Medicine, Beth Israel Deaconess Medical Center and Harvard Medical School, Boston, Massachusetts; the Department of Biological Chemistry and Molecular Pharmacology,§ Harvard Medical School, Boston, Massachusetts; the Harvard-Massachusetts Institute of Technology Division of Health Sciences and Technology,¶ Boston, Massachusetts; the Department of Surgery,‖ University of Kansas School of Medicine, Wichita, Kansas; and the Lung Biology Center,** University of California San Francisco, San Francisco, California*

The transforming growth factor (TGF)-β-inducible integrin αvβ6 is preferentially expressed at sites of epithelial remodeling and has been shown to bind and activate latent precursor TGF-β. Herein, we show that αvβ6 is overexpressed in human kidney epithelium in membranous glomerulonephritis, diabetes mellitus, IgA nephropathy, Goodpasture's syndrome, and Alport syndrome renal epithelium. To assess the potential regulatory role of αvβ6 in renal disease, we studied the effects of function-blocking αvβ6 monoclonal antibodies (mAbs) and genetic ablation of the β6 subunit on kidney fibrosis in Col4A3$^{-/-}$ mice, a mouse model of Alport syndrome. Expression of αvβ6 in Alport mouse kidneys was observed primarily in cortical tubular epithelial cells and in correlation with the progression of fibrosis. Treatment with αvβ6-blocking mAbs inhibited accumulation of activated fibroblasts and deposition of interstitial collagen matrix. Similar inhibition of renal fibrosis was observed in β6-deficient Alport mice. Transcript profiling of kidney tissues showed that αvβ6-blocking mAbs significantly inhibited disease-associated changes in expression of fibrotic and inflammatory mediators. Similar patterns of transcript modulation were produced with recombinant soluble TGF-β RII treatment, suggesting shared regulatory functions of αvβ6 and TGF-β. These findings demonstrate that αvβ6 can contribute to the regulation of renal fibrosis and suggest this integrin as a potential therapeutic target. ***(Am J Pathol 2007, 170:110–125; DOI: 10.2353/ajpath.2007.060158)***

Progressive fibrosis is a common process leading to the development of end-stage renal disease and promoted by epithelial remodeling, fibroblast activation, inflammation, and reorganization of cellular interactions with the extracellular matrix (ECM). Molecular mechanisms contributing to these events are complex and include misregulation of the transforming growth factor (TGF)-β axis, aberrant ECM remodeling, and altered expression and function of cell adhesion receptors of the integrin superfamily.[1–5] Recent studies have revealed important regulatory functions of several integrins and associated molecules in renal epithelial and mesenchymal cells.[3,6–8]

Among the integrins whose expression is strongly increased in renal disease is the TGF-β-inducible integrin αvβ6.[5,9,10] αvβ6 expression is generally restricted to epithelial cells where it is expressed at low levels in normal adult tissues and elevated during development, injury, and neoplasia.[9,11–13] Although αvβ6 is expressed at relatively low levels in healthy adult kidney, its expression is prominent in the developing mouse kidney, particularly in the proximal tubules, loop of Henle, and collecting

Supported in part by National Institutes of Health/National Institute of Diabetes and Digestive and Kidney Diseases grant DK 55001 (to R.K.).

K.H. and M.E.L. contributed equally to the manuscript.

Accepted for publication September 13, 2006.

Supplemental material for this article can be found on *http://ajp.amjpathol.org*.

Address reprint requests to Shelia M. Violette, Biogen Idec, 12 Cambridge Center, Cambridge, MA 02142. E-mail: shelia.violette@biogenidec.com.

ducts.[11,12,14] Recently, elevated expression of αvβ6 has been reported for various forms of human kidney pathology.[10]

Consistent with the increased expression of αvβ6 *in vivo* during tissue remodeling, expression of the αvβ6 integrin in cultured epithelial cells can be induced by cytokines that regulate epithelial remodeling, including EGF and TGF-β.[5,9] Moreover, overexpression of β6 in the skin of transgenic mice has been shown to provoke formation of spontaneous chronic wounds,[15] suggesting that αvβ6 may play an important role in regulating epithelial tissue remodeling.

Known ligands for αvβ6 include fibronectin, tenascin, and the latency-associated peptides 1 and 3 (LAP1 and LAP3), the N-terminal fragments of the latent precursor forms of TGF-β1 and -β3.[16–19] As a result of binding to these ligands, αvβ6 can mediate cell adhesion, spreading, migration, and activation of latent TGF-β. TGF-β is synthesized as a latent protein that is cleaved and secreted with the N-terminal LAP noncovalently associated with the mature active C-terminal TGF-β cytokine. The latent TGF-β complex cannot bind to its cognate receptor and thus remains biologically inactive until converted to the active form by one of several alternative mechanisms that include cleavage by proteases, exposure to low pH or ionizing radiation, and conformational changes in the latent complex, allowing it to bind to its cognate receptors.[20–22] An activating conformational change can be induced by αvβ6 involving direct binding of the integrin to an RGD motif contained within LAP1 and LAP3. This binding converts the TGF-β precursor into a receptor binding-competent state.[17,19] These findings suggest that up-regulation of αvβ6 expression on the surface of epithelial cells can lead to local TGF-β activation followed by paracrine activation of TGF-β-dependent events in bystander cells. This would include the possibility for indirect downstream effects on TGF-β activity that could be mediated by altering inflammation and fibrosis initially at sites of αvβ6 expression.

Because TGF-β has been implicated as a central regulator of renal fibrosis, we hypothesized that its local activation by αvβ6 may be an important process in the onset and progression of renal disease and blockade of αvβ6 function could suppress the development of kidney fibrosis. In the studies described herein, we show that αvβ6 is highly up-regulated in a mouse model of kidney fibrosis and in human kidney samples with fibrotic pathology. Using Col4A3$^{-/-}$ mice, a model of progressive kidney disease similar to that observed in the human Alport syndrome, we show that monoclonal antibodies (mAbs) blocking the ligand binding and TGF-β activation functions of αvβ6,[23] as well as genetic ablation of β6, potently inhibit both glomerular and tubulointerstitial fibrosis and delay destruction of kidney tissue architecture. We show that although the αvβ6 integrin has restricted expression in the kidney to tubular epithelial cells, it can provide protective effects at distal sites in the tissue. These findings raise the possibility that the antifibrotic effects may also be mediated in part via indirect extrarenal effects in addition to direct effects of blocking αvβ6 on tubular epithelial cells. Delayed treatment studies indicate that therapeutic blockade of αvβ6 not only inhibits the progression of kidney fibrosis but has the potential to allow resolution of existing fibrotic lesions. Our analysis of molecular signatures associated with kidney disease progression and affected by αvβ6 inhibition indicates that the therapeutic impact of the αvβ6 blocking antibodies is similar to that of systemic TGF-β blockade and is mechanistically related to decreased TGF-β activity. These data suggest that αvβ6 is involved in the regulation of renal fibrosis and could provide a novel molecular target for its therapeutic modulation.

Materials and Methods

Antibodies and Reagents

αvβ6 mAbs were generated as previously described.[23] Human/mouse chimeric 2A1 and 3G9 cDNAs were generated from the respective parent hybridoma total RNAs with constant region primers CDL-739 for the heavy chain and CDL-738 for the light chain using the First Strand cDNA synthesis kit (Amersham/Pharmacia, Piscataway, NJ). The heavy and light chain variable regions were amplified by the polymerase chain reaction using the same 3′ primers used for cDNA synthesis and pools of degenerate primers specific for most murine antibody gene signal sequences (sequences available on request) and Pfu DNA polymerase (Stratagene, La Jolla, CA). Cloned heavy and light chain variable regions were ligated into mammalian expression vectors with human IgG1 constant regions. Recombinant soluble murine TGF-β receptor type II-Ig fusion protein (rsTGF-βRII-Ig) was generated as previously described[7] and purchased from R&D Systems (532-R2; Minneapolis, MN). Antibodies were purchased as indicated: fluorescein isothiocyanate-conjugated pan anti-cytokeratin mAb (C-11; F3418) from Sigma-Aldrich (St. Louis, MO); anti-laminin B1 chain mAb (LT3; MAB1928) from Chemicon (Temecula, CA); phycoerythrin (PE)-conjugated anti-αv mAb (RMV7; CBL1346P) from Chemicon; rabbit anti-αv from Chemicon (AB1930); PE-rat IgG1 (553925) from BD Biosciences (San Jose, CA); and anti-smooth muscle actin (SMA)-Cy3 from Sigma-Aldrich (C-6198). We identified rabbit polyclonal anti-TGF-β (sc-146; Santa Cruz Biotechnology, Santa Cruz, CA) as an antibody that preferentially binds xenograft sections of 293 cells expressing a constitutively active form of TGF-β compared with xenograft sections of 293 cells expressing latent TGF-β.[24]

Flow Cytometry

Murine NIH3T3 cells stably transfected with β6 (NIH3T3b6) were generated as previously described.[23] Cells were harvested by trypsinization, washed in phosphate-buffered saline (PBS), and resuspended in flow cytometry (FC) buffer (1× PBS, 2% FBS, 0.1% NaN_3, 1 mmol/L $CaCl_2$, and 1 mmol/L $MgCl_2$). Cells (0.2×10^5) were incubated on ice for 1 hour in FC buffer containing purified primary antibodies in a total volume of 100 μl. After incubation, cells were washed two times with ice-

cold FC buffer and resuspended in 100 μl of FC buffer containing 5 μg/ml PE-conjugated donkey anti-mouse IgG (Jackson ImmunoResearch) and incubated on ice for 30 minutes. For monitoring αv expression, cells were incubated with a PE-conjugated rat anti-mouse αv mAb (RMV-7) and a PE-conjugated rat IgG1 control. Cells were washed two times with ice-cold FC buffer, and binding of the labeled secondary antibody was monitored by flow cytometry.

Immunohistochemistry

Tissue sections were deparaffinized in xylene and ethanol, rehydrated in distilled water, and then immersed in methanol containing 0.45% H_2O. Tissues were incubated with pepsin (00-3009; Zymed, San Francisco, CA) and blocked with avidin and biotin (SP-2001; Vector Laboratories, Burlingame, CA). Primary antibody was diluted in PBS containing 0.1% bovine serum albumin, and tissues were incubated overnight at 4°C. For immunostaining β6 on mouse tissue, sections were incubated with a human/mouse chimeric form of the anti-αvβ6 mAb, 2A1,[23] and an anti-human biotinylated secondary antibody (PK-6103; Vector Laboratories). For immunostaining β6 on human tissue, sections were incubated with murine 2A1,[23] and an anti-mouse-biotinylated secondary antibody (PK-6102; Vector Laboratories). Avidin-biotin complex-horseradish peroxidase (Vector kit PK-6102) was applied to sections and incubated for 30 minutes at room temperature, and 3,3′-diaminobenzidine substrate was prepared as directed (SK-4100; Vector Laboratories) and applied to sections for 5 minutes at room temperature. Tissue sections were stained with Mayer's hematoxylin for 1 minute and rinsed in water and PBS.

Frozen tissue sections embedded in O.C.T. compound (Sakura, Tokyo, Japan) were fixed in acetone and blocked with 0.5% casein/0.05% thimerosal in PBS. For immunostaining β6 on human tissue, sections were incubated with murine 2A1[23] and an anti-mouse Alexa Fluor 594 secondary antibody (A-11032; Molecular Probes, Eugene, OR). For immunostaining β6 on mouse tissue, sections were incubated with a human/mouse chimeric form of 2A1 and an anti-human Alexa Fluor 594-conjugated secondary antibody (A-11014; Molecular Probes). For laminin and αv immunostaining, an anti-rat Alexa Fluor 488-conjugated secondary antibody (A-11006; Molecular Probes) was used. All other antibodies were directly conjugated as indicated previously. All images were taken at ×20 with the exception of Figure 2A, which was taken at ×40. All human tissue samples were obtained under approval of local institutional review and patient approval.

Quantitation of SMA Immunostaining, Tubular Damage, and Interstitial Fibrosis

SMA immunostaining area was quantitated using MetaMorph v5.0 (Universal Imaging Corporation, Sunnyvale, CA) and expressed as percent area relative to total image size. For SMA immunostaining, ×20 images from at least five cortical and one to two medullary sections from each animal were analyzed. Statistical analysis of treatment groups was performed using analysis of variance. Tubular damage and interstitial volume were assessed as previously described[25,26] with modifications. In brief, ×20 images were taken from sections stained with Trichrome-Masson. A grid containing 117 points (13 × 9) was set up 35 μm apart in Stereo Investigator 6.5 (MBF Bioscience, Williston, VT). The number of grid points overlying healthy appearing tubules (healthy tubule volume index) and degenerated tubules and interstitial space (interstitial volume index) was counted and expressed as a percentage of all sampling points. For tubular dilation index, the number of dilated tubules per image was counted. For each kidney, 10 randomly selected, nonoverlapping fields were analyzed by a blinded observer.

Treatment of Col4A3$^{-/-}$ Mice with mAbs and rsTGF-βRII-Ig

Col4A3$^{+/-}$ mice in a 129Sv/J background were bred to generate Col4A3$^{-/-}$ mice. Mice were injected intraperitoneally with proteins three times a week from 3 weeks of age to 7 or 8.5 weeks of age, as indicated. mAbs were injected intraperitoneally at 4 mg/kg, and rsTGF-βRII-Ig was injected at 2 mg/kg. Mice were euthanized, and kidneys were collected for RNA and immunostaining. All animal studies were approved and performed in accordance with the Institutional Animal Care and Use Committee.

Total RNA Purification and cDNA Synthesis

Kidneys were homogenized directly into TRIzol (155-96-018; Invitrogen, Carlsbad, CA), and RNA was extracted according to manufacturer's protocol with an additional 1 ml of acidic phenol/chloroform/isoamyl alcohol (25:24:1, pH 6.6) extraction. Purified total RNA was resuspended in diethylpyrocarbonate-treated H_2O (Ambion Inc., Austin, TX) and 260 and 280 recorded (Spectra max Plus; Molecular Devices, Sunnyvale, CA). Residual DNA was removed using 5 units of DNase I amplification grade (Invitrogen) at 20°C for 15 minutes. cDNA was generated using a high-capacity cDNA archive kit according to the manufacturer's protocol (Applied Biosystems Inc., Foster City, CA).

Design of Primers, Probes, and Oligonucleotide Standard Templates for Taqman

Oligonucleotide primers and Taqman MGB probes were designed from Affymetrix consensus sequences using Primer Express version 2.0.0 (Applied Biosystems Inc.). Taqman MGB probes were designed with a 5′ covalently linked fluorescent reporter dye (FAM) and a minor groove binder/nonfluorescent quencher covalently linked to the 3′ end. Oligonucleotide standard templates were designed by the addition of 10 bp of gene-specific se-

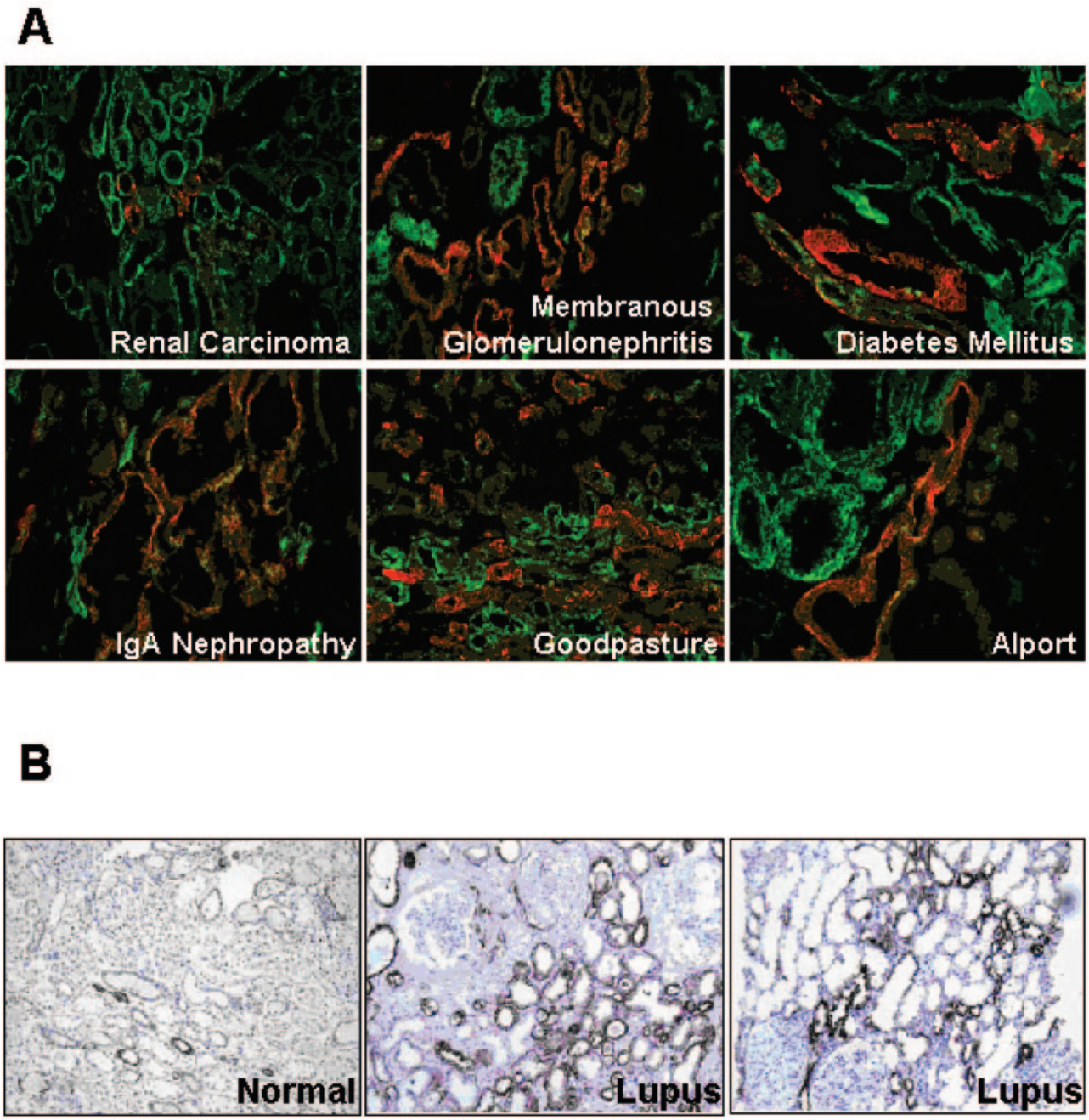

Figure 1. αvβ6 immunostaining in human kidney disease. **A:** Frozen human kidney sections immunostained with an αvβ6 mAb (red) and a pan-cytokeratin mAb (green). All images were taken at the same magnification. **B:** Paraffin-embedded human kidney sections immunostained with an αvβ6 mAb.

quence to the 5′ and 3′ ends of the amplicon. Reverse-phase high-performance liquid chromatography-purified primers and oligonucleotide standard templates were purchased from Biosearch Technologies Inc. (Novato, CA). High-performance liquid chromatography-purified primers and probe for murine glyceraldehyde-3-phosphate dehydrogenase were synthesized at Biogen Idec (5′-CATGGCCTTCCGTGTTCCTA-3′, 5′-GCGGCACGTCAGATCC-3′, and 6FAM-5′-CCCCAATGTGTCCGTC-3′).

Taqman Thermal Cycling

Quadruplicate polymerase chain reactions for samples and standards were cycled in a 7900HT thermal cycler (Applied Biosystems Inc.) under the following conditions: 50°C for 2 minutes (uracil *N*-deglycosylase digest), 95°C for 10 minutes (activation of *Taq* thermostable polymerase), and 40 cycles of 95°C for 15 seconds and 60°C for 60 seconds. The fluorescence emission was collected every 7 seconds for the length of the run for each reaction

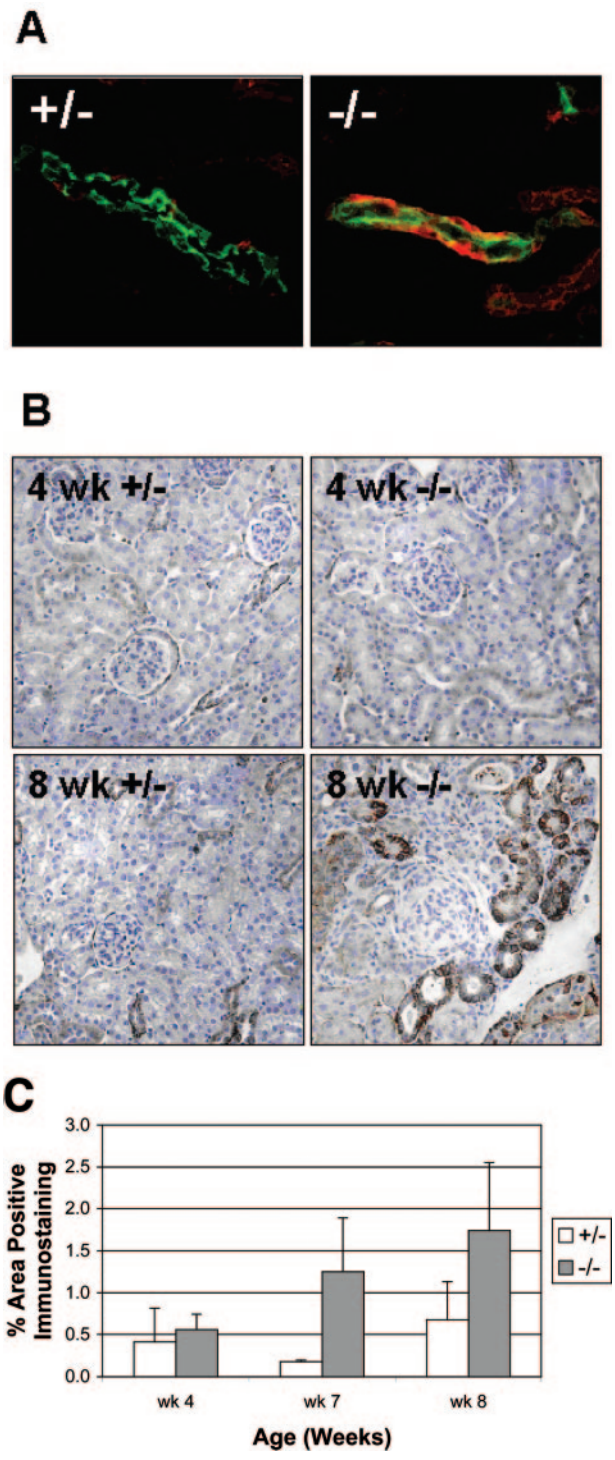

Figure 2. $\alpha v\beta 6$ immunostaining in Col4A3$^{+/-}$ and Col4A3$^{-/-}$ mouse kidneys. **A:** Frozen kidney sections from 7-week-old Col4A3$^{+/-}$ mice and Col4A3$^{-/-}$ mice immunostained with an $\alpha v\beta 6$ mAb (red) and a pan-cytokeratin mAb (green). **B:** Paraffin-embedded kidney sections from 4- and 8-week-old Col4A3$^{+/-}$ and Col4A3$^{-/-}$ mice immunostained with an $\alpha v\beta 6$ mAb. **C:** Quantitation of $\alpha v\beta 6$ immunostaining in kidneys from 4-, 7-, and 8-week-old Col4A3$^{+/-}$ and Col4A3$^{-/-}$ mice ($n = 3$).

well. Relative transcript quantities were determined for each sample by comparison with oligonucleotide standard curve using Sequence Detection Software (Applied Biosystems Inc.).

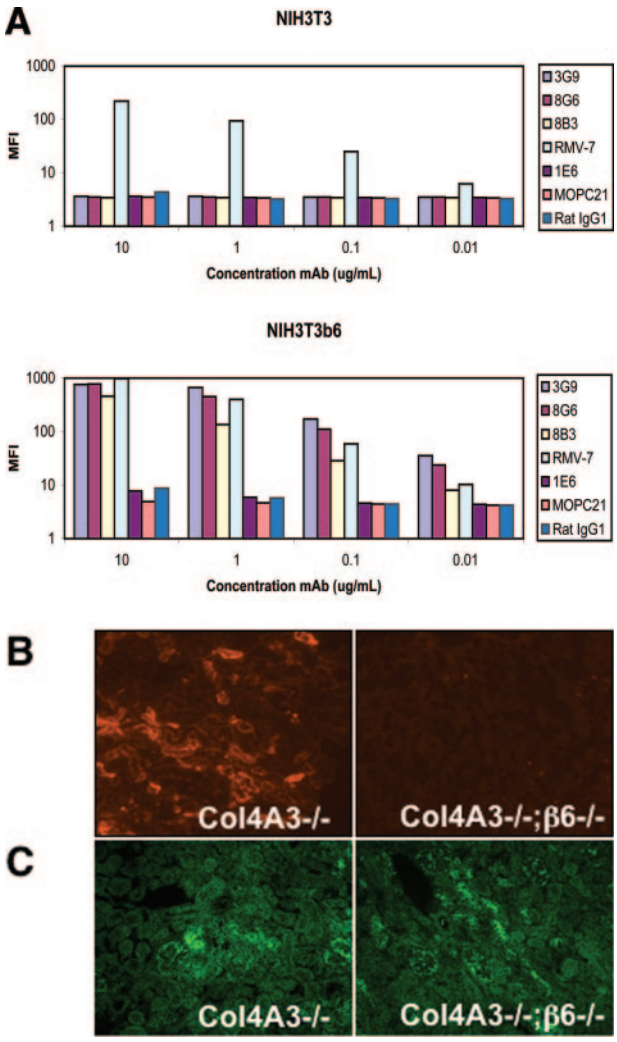

Figure 3. Specificity of $\alpha v\beta 6$ mAb binding. **A:** Flow cytometry analysis of $\alpha v\beta 6$ mAbs (3G9, 8G6, and 8B3), anti-αv mAb (RMV-7), negative control mAbs (1E6 and MOPC21), and isotype control (rat IgG1) binding to NIH3T3 cells and NIH3T3b6 cells. **B:** Immunostaining Col4A3$^{-/-}$ and Col4A3$^{-/-}$; $\beta 6^{-/-}$ kidney sections with anti-$\alpha v\beta 6$ mAb (human/mouse chimeric 3G9). **C:** Immunostaining Col4A3$^{-/-}$ and Col4A3$^{-/-}$;$\beta 6^{-/-}$ kidney sections with anti-αv polyclonal antibody.

Microarray Procedures

Total RNA was isolated from kidney samples of each experimental group of mice (five animals per group). The quality of the resulting RNA preparations was verified by capillary electrophoresis on Bioanalyzer 2000 (Agilent). Experimental groups of Col4A3$^{-/-}$ mice analyzed included no treatment, or treatment with one of the following proteins: negative control mAb 1E6, nonblocking anti-$\alpha v\beta 6$ mAb 8B3, blocking anti-$\alpha v\beta 6$ mAb 3G9, blocking anti-$\alpha v\beta 6$ mAb 8G6, and rsTGFβRII-Ig. Additional control groups included wild-type mice of the same genetic background treated with 3G9 and naive wild-type mice. Hybridization probes were prepared from each of the RNA samples and profiled on separate U74Av2 Gene Chip oligonucleotide arrays (Affymetrix, Santa Clara, CA). Hybridization probe synthesis, hybridization, and microarray scanning were performed using the manufacturer's protocols. The array scans were converted into Af-

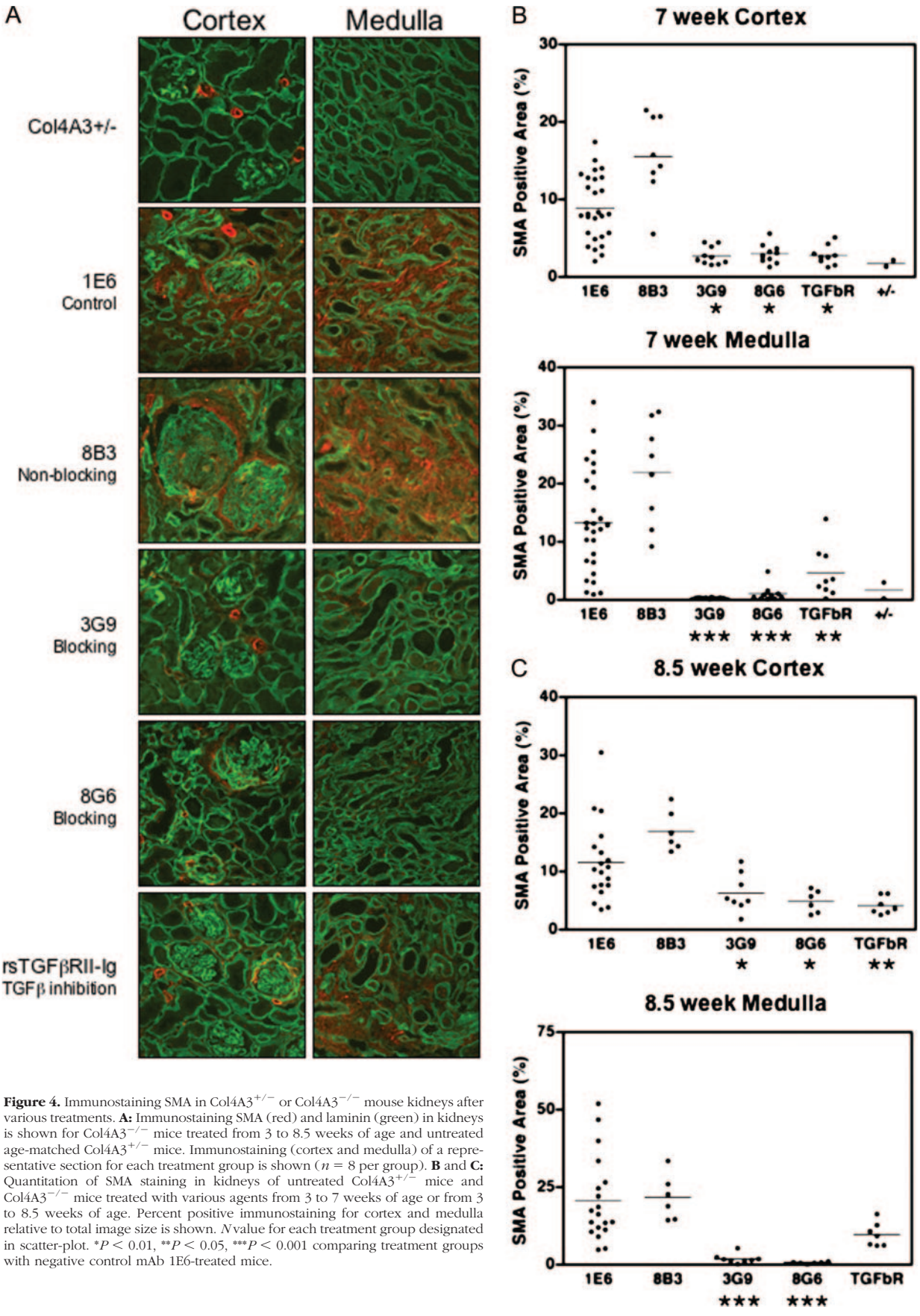

Figure 4. Immunostaining SMA in Col4A3$^{+/-}$ or Col4A3$^{-/-}$ mouse kidneys after various treatments. **A:** Immunostaining SMA (red) and laminin (green) in kidneys is shown for Col4A3$^{-/-}$ mice treated from 3 to 8.5 weeks of age and untreated age-matched Col4A3$^{+/-}$ mice. Immunostaining (cortex and medulla) of a representative section for each treatment group is shown ($n = 8$ per group). **B** and **C:** Quantitation of SMA staining in kidneys of untreated Col4A3$^{+/-}$ mice and Col4A3$^{-/-}$ mice treated with various agents from 3 to 7 weeks of age or from 3 to 8.5 weeks of age. Percent positive immunostaining for cortex and medulla relative to total image size is shown. *N* value for each treatment group designated in scatter-plot. $^{*}P < 0.01$, $^{**}P < 0.05$, $^{***}P < 0.001$ comparing treatment groups with negative control mAb 1E6-treated mice.

fymetrix.CEL files, and the resulting data set (group of CEL files representing the complete experiment) was normalized using the robust microarray average method. Statistical and clustering analyses were done using the GeneSpring (Agilent) and Spotfire (Spotfire) data mining tools. We used a Two-strp analysis of variance and fold-change filtering to identify probe sets whose signal intensity was altered by experimental treatment compared with the untreated Col4A3$^{-/-}$ group at $P < 0.05$ and at least by twofold. Likewise, disease-associated transcripts were selected for differential expression between untreated Col4A3$^{-/-}$ and naive wild-type groups using the statistical cutoff of $P < 0.01$ and the signal fold-change cutoff of 2. The profiles of the resulting group of genes and the grouping of experimental conditions were analyzed and visualized by hierarchical clustering. Virtual pathway analysis was performed using the Ingenuity Pathway Analysis database (Ingenuity Systems).

Results

Expression of αvβ6 in Human Kidney Samples with Fibrotic Pathology

Several different types of human kidney disease, associated with inflammatory/fibrotic pathology, have shown a corresponding increased expression of TGF-β in the kidney tissue.[27–29] Using immunohistochemical analysis, we examined the expression of αvβ6 in human kidney biopsy samples associated with chronic inflammation and fibrosis as a potential mechanism leading to increased activation of TGF-β (Figure 1, A and B). Tissue samples from membranous glomerulonephritis, diabetes mellitus, IgA nephropathy, Goodpasture's syndrome, Alport syndrome, and lupus all showed prominent αvβ6 staining in the epithelial lining of dilated and damaged tubules. In contrast, samples of morphologically normal kidneys (renal carcinoma and normal tissue), showed minimal occasional immunostaining in tubules. Glomerular staining was absent in all kidney samples analyzed. This finding is consistent with previous reports that αvβ6 is expressed at low levels in healthy adult epithelium but is up-regulated during tissue injury and repair.[10,11,13,15,17]

Expression of αvβ6 in the Kidneys of Col4A3$^{-/-}$ Mice Correlates with Progression of Kidney Fibrosis

Col4A3$^{-/-}$ mice, a mouse model of human Alport disease, develop progressive glomerulonephritis leading to the accumulation of ECM in both the glomerular and interstitial regions of the kidney accompanied by increased expression of a number of standard markers of fibrosis.[30,31] It has been previously reported that treatment of Col4A3$^{-/-}$ mice with rsTGF-βRII-Ig leads to inhibition of kidney fibrosis.[7] Kidneys from Col4A3$^{-/-}$ mice begin to show histological signs of fibrosis at approximately 5 to 6 weeks of age. The disease progresses rapidly with age, and the mice die of renal failure at approximately 11 weeks. Heterozygous Col4A3$^{+/-}$ mice do not develop glomerulonephritis, and their kidneys are histologically indistinguishable from those of wild-type littermates. To examine the dynamics of αvβ6 expression in kidneys of Col4A3$^{+/-}$ and Col4A3$^{-/-}$ (Alport) mice of increasing age, we performed immunohistochemical analysis of αvβ6 expression in kidneys isolated from 4-, 7-, and 8-week-old mice (Figure 2, A–C). At 4 weeks of age, there was occasional expression of αvβ6 in kidney tubules of Col4A3$^{+/-}$ and Col4A3$^{-/-}$ mice. By 7 weeks, expression of αvβ6 was markedly increased in tubular epithelial cells of Col4A3$^{-/-}$ mice but not in the Col4A3$^{+/-}$ kidneys. This increased expression of αvβ6 was persistent in the Col4A3$^{-/-}$ mice beyond 8 weeks of age. We also observed an increase in the intensity of αvβ6 staining in the epithelial cells of dilated and damaged tubules in Col4A3$^{-/-}$ (Alport) mice after 6 weeks of age. Quantitative analysis of αvβ6 immunostaining in kidneys ($n = 3$) showed an increase in the area of immunostaining in Col4A3$^{-/-}$ compared with Col4A3$^{+/-}$ mice but did not reach statistical significance. The increased expression during the period of 7 to 8 weeks of age coincided with rapid progression of kidney fibrosis in Col4A3$^{-/-}$ mice. In contrast, minimal αvβ6 expression and a slightly detectable age-dependent increase of its intensity of immunostaining were detected in the kidneys of Col4A3$^{+/-}$ mice throughout the time course. Because the expression of αvβ6 in kidneys of Col4A3$^{-/-}$ mice correlated with progression of fibrosis, we determined whether blockade of αvβ6 function could inhibit the initiation and progression of fibrotic lesions.

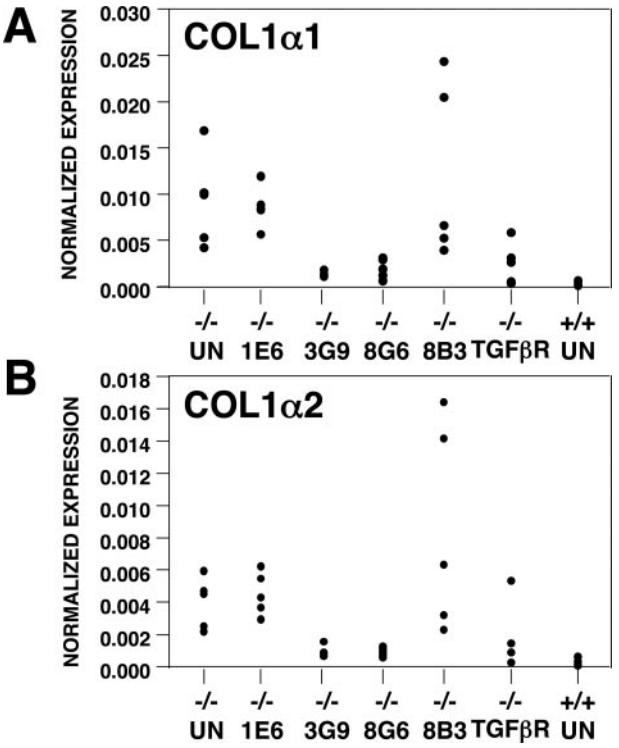

Figure 5. Taqman analysis of collagen 1α1 (**A**) and collagen 1α2 (**B**) mRNA levels. RNA was isolated from kidneys of 7-week-old untreated or treated Col4A3$^{-/-}$ mice and 7-week-old untreated Col4A3$^{+/+}$ mice.

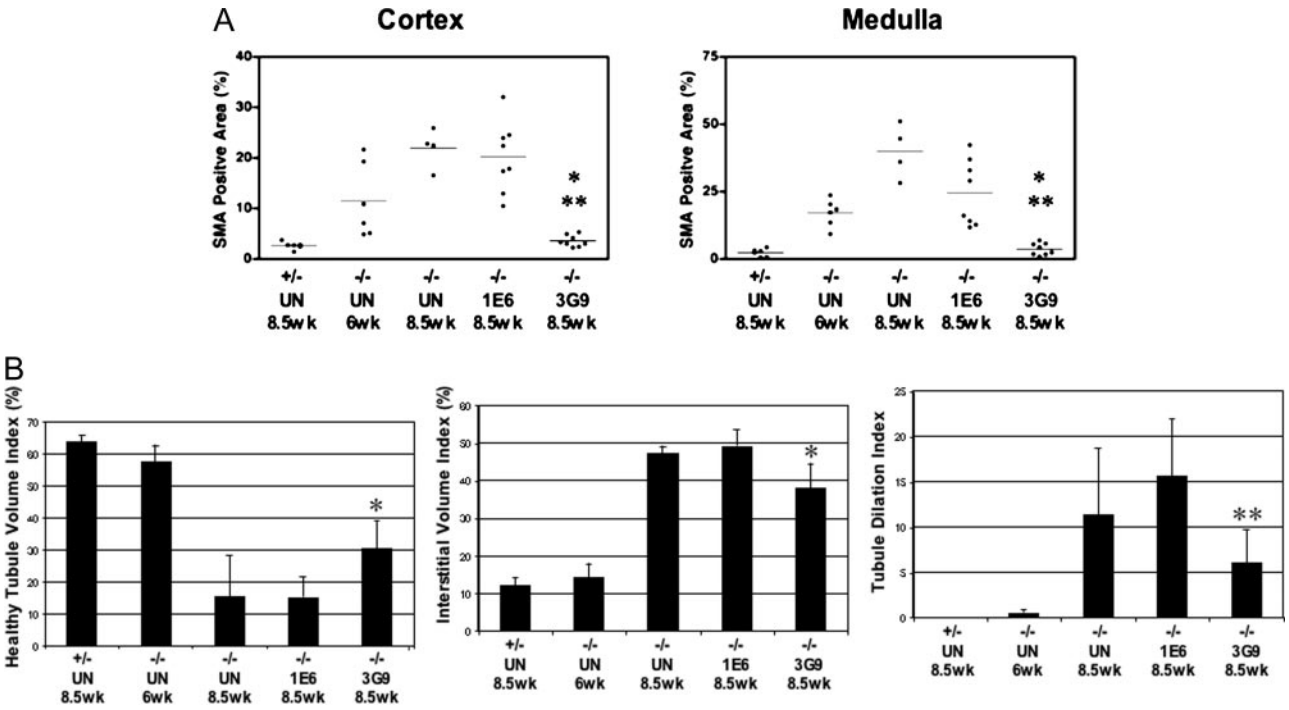

Figure 6. Quantitation of SMA immunostaining and healthy tubule area in kidneys from Col4A3$^{-/-}$ kidneys with delayed 3G9 mAb treatment. **A:** SMA immunostaining in kidneys from untreated 8.5-week-old Col4A3$^{+/-}$ mice, untreated 6-week-old Col4A3$^{-/-}$ mice, untreated 8.5-week-old Col4A3$^{-/-}$ mice, and 8.5-week-old Col4A3$^{-/-}$ mice treated with 1E6 and 3G9 from 6 to 8.5 weeks of age were quantitated. *N* value for each treatment group designated in scatter plot. *$P < 0.0005$, comparing 3G9 treatment group with negative control mAb 1E6-treated Col4A3$^{-/-}$ mice. **$P < 0.02$ comparing 3G9 treatment group with untreated 6-week-old Col4A3$^{-/-}$ mice. **B:** Quantitation of area of healthy tubules (healthy tubule volume index), area of degenerated tubules and interstitial space (interstitial volume index), and number of dilated tubules (tubular dilation index). *$P < 0.001$, and **$P < 0.002$ comparing 3G9 treated with negative control mAb 1E6-treated Col4A3$^{-/-}$ mice.

Specificity of mAbs Binding to αvβ6 in the Kidneys of Col4A3$^{-/-}$ Mice

We have previously reported the generation of potent and selective anti-αvβ6 mAbs,[23] including mAbs that bind to αvβ6 without affecting its ability to bind ligands (nonblocking mAbs) and mAbs that that block both ligand binding and αvβ6-mediated TGF-β activation (blocking mAbs). To verify that αvβ6 blocking mAbs used for *in vivo* studies were selective for binding to the αvβ6 integrin, we performed fluorescence-activated cell sorting analysis (Figure 3A) comparing the binding of the αvβ6 mAbs to untransfected parent NIH3T3 cells and to NIH3T3 cells transfected with murine β6 cDNA (NIH3T3b6). Although a control anti-αv mAb, RMV7, stained both untransfected and αvβ6-expressing NIH3T3 cells, the anti-αvβ6 mAbs selectively bound only NIH3T3b6 cells. To confirm specificity of binding αvβ6 in kidneys, we generated a human/mouse chimeric form of one of the blocking αvβ6 mAbs, 3G9, and compared the pattern of immunostaining produced with a rabbit anti-αv polyclonal antibody (Figure 3, B and C). The chimeric and the original murine form of 3G9 had comparable target binding affinities as determined by fluorescence-activated cell sorting and enzyme-linked immunosorbent assay (data not shown). The chimeric form of 3G9 specifically immunostained tubular epithelial cells in kidneys of Col4A3$^{-/-}$ mice and showed no immunostaining of kidney sections from Col4A3$^{-/-}$ crossed with β6$^{-/-}$ mice (Col4A3$^{-/-}$;β6$^{-/-}$). Immunostaining of kidneys with the anti-αv antibody revealed no significant differences between the Col4A3$^{-/-}$ mice or Col4A3$^{-/-}$;β6$^{-/-}$ mice.

Treatment of Col4A3$^{-/-}$ (Alport) Mice with Anti-αvβ6 mAbs Inhibits Kidney Fibrosis

To determine the potential functional involvement of αvβ6 in the regulation of kidney fibrosis, we have tested the ability of blocking αvβ6 mAbs to affect the initiation and progression of advanced fibrotic lesions. To assess the preventive effects of αvβ6 blockade, Col4A3$^{-/-}$ mice were treated from 3 to 7 weeks of age or from 3 to 8.5 weeks of age with two different blocking αvβ6 mAbs, 3G9 or 8G6; a nonblocking αvβ6 mAb, 8B3; or an isotype-matched negative control mAb, 1E6. For phenotypic reference and to monitor the effects of systemic TGF-β inhibition, these studies also included Col4A3$^{-/-}$ mice treated with rsTGFβRII-Ig. Kidneys were collected for histological evaluation and for isolation of RNA. Histological hallmarks of fibrosis and SMA expression were dramatically increased in the Col4A3$^{-/-}$ kidneys at 7 and 8.5 weeks compared with kidneys from age-matched Col4A3+/− mice. Kidneys from negative control mAb-treated Col4A3$^{-/-}$ mice presented with an expanded and fibrotic glomerular mesangium and a crescent formation in the Bowman's capsule (Figure 4A, 1E6). These kidneys also showed marked myofibroblast activation

and interstitial fibrosis that was associated with tubular epithelial injury and dilation. Treatment of Col4A3$^{-/-}$ mice with blocking $\alpha v\beta 6$ mAbs 3G9 or 8G6 markedly reduced glomerular and interstitial injury and fibrosis, resulting in considerable gross preservation of kidney architecture (Figure 4A, 3G9 and 8G6). These effects of the blocking $\alpha v\beta 6$ mAbs were accompanied by reduction of SMA expression by >65% in the glomeruli and by >90% in the interstitial regions (Figure 4, B and C). The effect of the blocking mAbs on SMA expression in the glomeruli suggest that although the expression of the $\alpha v\beta 6$ integrin is restricted to tubular epithelial cells, blocking its function can have effects at more distal sites in the tissue, which could be mediated at least in part due to indirect systemic effects of the blocking $\alpha v\beta 6$ mAbs. No effect on the progression of fibrosis was seen in kidneys of Col4A3$^{-/-}$ mice injected with the nonblocking $\alpha v\beta 6$ mAb, 8B3. Consistent with previously reported inhibition of kidney fibrosis via blockade of TGF-β,[7,32–35] treatment of Col4A3$^{-/-}$ mice with rsTGFβRII-Ig produced inhibition of renal fibrosis similar to that produced by the blocking $\alpha v\beta 6$ mAbs, as judged by changes in histological appearance and SMA content of the kidney tissues. The effects of $\alpha v\beta 6$ blocking mAbs on SMA expression were paralleled by reduction in total kidney tissue levels of collagen1α1 and collagen1α2 mRNA (Figure 5, A and B). Treatment of the Col4A3$^{-/-}$ mice with 3G9, 8G6, or rsTGF-βRII-Ig caused a significant reduction of collagen1α1 and collagen1α2 mRNA abundance, whereas the nonblocking $\alpha v\beta 6$ mAb and isotope control mAb had no significant effect on the levels of these transcripts.

To test the impact of $\alpha v\beta 6$ blockade on advanced renal fibrosis, we have studied the effects of $\alpha v\beta 6$ blocking mAbs on kidney fibrosis in 6-week-old Col4A3$^{-/-}$ mice, at which time kidney pathology is manifested by measurable injury and accumulation of SMA-positive activated fibroblasts. Mice were treated with the $\alpha v\beta 6$ blocking mAb 3G9 or with isotype control mAb 1E6 for 2.5 weeks and then sacrificed at 8.5 weeks of age. Quantitation of SMA immunostaining revealed a decrease in the presence of SMA-positive fibroblasts in the kidneys from Col4A3$^{-/-}$ mice treated with 3G9 compared with isotype control mAb-treated mice (Figure 6A). Of equal importance, the intensity and area of SMA immunostaining with delayed 3G9 treatment was diminished compared with the level of SMA observed at the onset of treatment (6 weeks), suggesting that therapeutic blockade of $\alpha v\beta 6$ can inhibit the progression of kidney fibrosis and has the potential to allow resolution of existing fibrotic lesions. Consistent with a decrease in SMA staining, treatment with 3G9 induced a marked reversion in pathology compared with 1E6 treatment. This was measured as an increase in the area of healthy tubules (healthy tubule volume index), a decrease in the interstitial area (interstitial volume index), and a reduction in the number of dilated tubules (tubule dilation index) (Figure 6B). Collectively, these findings indicate that the kidney architecture was better preserved and that there was a significant reduction in fibrosis by treatment with an $\alpha v\beta 6$ blocking mAb.

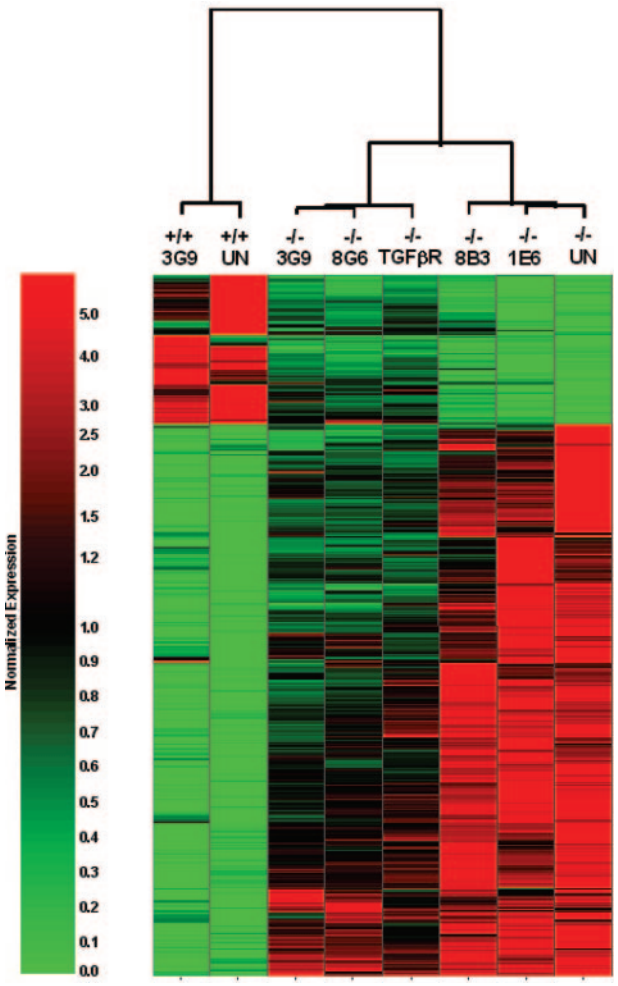

Figure 7. Patterns of gene expression and modulation in kidneys of 7-week-old Col4A3$^{-/-}$ mice. Shown are 395 GeneChip probe sets selected for twofold or greater variation between wild-type and untreated Col4A3$^{-/-}$ (UN) groups at $P < 0.01$. The columns of the heat map display patterns of relative gene expression levels for individual experimental groups. Each column represents 395 normalized mean probe set signal intensity values for a single experimental group of five mice. Changes in gene expression across the experimental conditions are reflected in the color variation as shown by the color bar. Two-dimensional hierarchical clustering was performed to explore relationships (shown by the dendrogram) among the experimental groups.

Regulation of Kidney Gene Expression by Anti-$\alpha v\beta 6$ mAbs

To gain further insight into disease mechanisms associated with $\alpha v\beta 6$ function, we have performed an Affymetrix GeneChip analysis of gene expression in kidney tissues from wild-type and Col4A3$^{-/-}$ mice. A group of genes with altered expression in Col4A3$^{-/-}$ kidneys was identified as 395 GeneChip probe sets showing at least twofold mean difference in normalized signal intensity comparing 7-week-old Col4A3$^{-/-}$ and age-matched wild-type kidneys at $P < 0.01$ (Figure 7; Supplementary Table 1, see *http://ajp.amjpathol.org*). Functional annotation of the differentially expressed genes was performed using the Ingenuity Pathway Analysis (IPA) tool and has indicated a predominant association of genes overexpressed in the Col4A3$^{-/-}$ kidneys with inflammation and

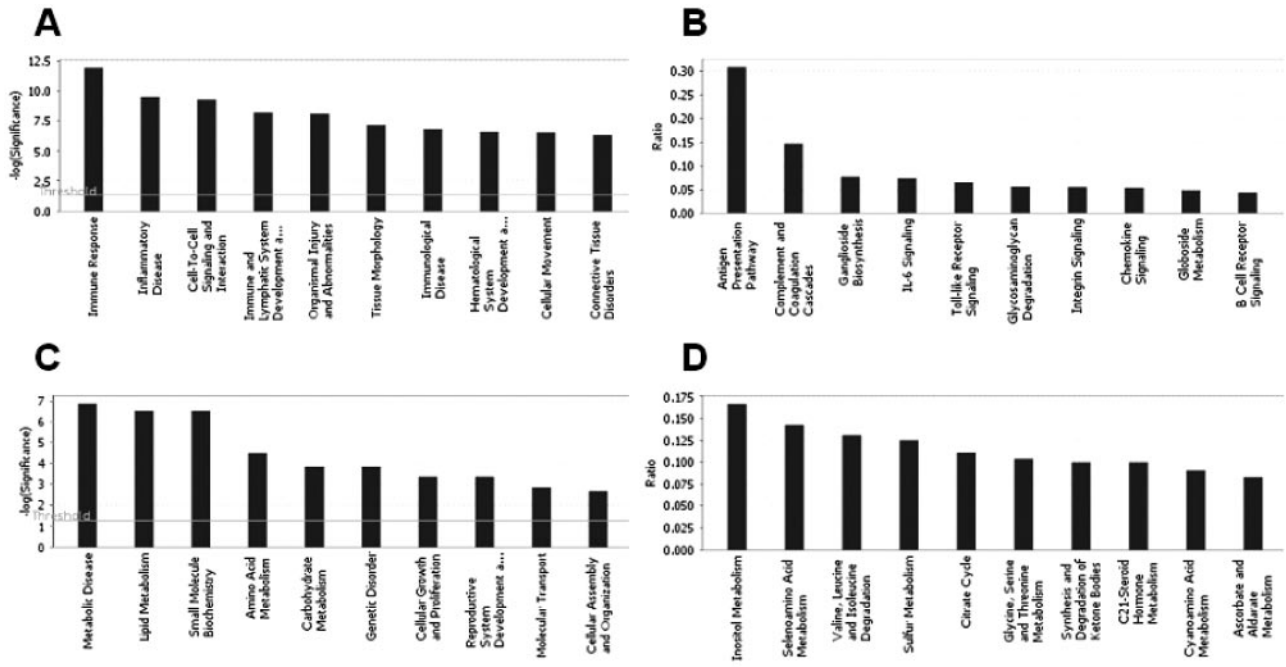

Figure 8. Functional annotation of αvβ6-dependent genes associated with renal disease in Col4A3$^{-/-}$ kidneys. IPA was performed separately on the lists of probe sets corresponding to genes over- or underexpressed in Col4A3$^{-/-}$ kidneys compared with wild type. The lists used for IPA were subsets of the 395 probe sets originally selected for significant (>2-fold, $P < 0.01$) variation between Col4A3$^{-/-}$ and wild-type groups. Shown are rank-ordered lists of biological functions (**A** and **C**) and canonical pathways (**B** and **D**) associated with genes overexpressed (**A** and **B**) and down-modulated (**C** and **D**) in 7-week-old Col4A3$^{-/-}$ kidneys.

regulation of leukocyte functions, whereas genes whose expression was decreased were associated primarily with metabolic regulation (Figure 8).

Treatment of mice with αvβ6-blocking mAbs 3G9 and 8G6 attenuated differential expression of a subset of genes in Col4A3$^{-/-}$ kidneys. We have used analysis of variance (Welch analysis of variance) to identify transcripts affected by the experimental treatments at $P <$ 0.05 and further filtered the resulting probe sets to select those showing at least a twofold difference in signal intensity in response to treatment. This procedure yielded 56, 42, and 28 probe sets significantly affected by 3G9, 8G6, and rsTGF-βRII-Ig, respectively (Supplementary Tables 2, 3, and 4, see *http://ajp.amjpathol.org*). These groups of probe sets showed considerable overlap, and each of the groups represented a fully included subset of the 395 corresponding transcripts differentially expressed in Col4A3$^{-/-}$ kidneys (Figure 9A). We observed similar modulation of gene expression by the two different αvβ6 blocking mAbs (Figures 7 and 9A; Supplementary Tables 2 and 3, see *http://ajp.amjpathol.org*) previously shown to belong to two different biochemical classes.[23] Neither the nonblocking anti-αvβ6 mAb 8B3 nor the isotype control mAb 1E6 had a significant effect on gene expression. Therefore, the impact of the αvβ6 mAbs on kidney gene expression was likely due to blockade of αvβ6 function rather than to activation of integrin signaling or to nonspecific events. We found no significant effects of the blocking αvβ6 mAb 3G9 on gene expression in normal wild-type kidney tissue. This observation suggested that the effects of the αvβ6-blocking mAbs observed in our experiments reflected primarily disease-specific regulatory functions of αvβ6.

To explore potential relationships of the genes modulated by αvβ6 blocking mAbs with major regulatory pathways, we subjected the respective gene lists to virtual regulatory network analysis using the IPA software (Figures 8 and 9). IPA compares gene lists provided as input to a curated database of known physical and regulatory interactions among genes and proteins. This analysis produces a ranked list and individual configurations of regulatory pathways that are most likely to be reflected by a given list of modulated genes. Although the lists of genes modulated by mAbs 3G9 and 8G6 were not completely identical (data not shown; Supplementary Tables 2 and 3, see *http://ajp.amjpathol.org*), IPA has revealed TGF-β-dependent networks as the highest-scoring regulatory networks affected by 3G9 (Figure 9B) and by 8G6 (Figure 9C). Consistent with this finding, hierarchical clustering of the mean gene expression profiles of the experimental groups has demonstrated similarity between patterns of gene modulation by αvβ6 blocking mAbs and by rsTGF-βRII-Ig (Figure 7).

Blockade of αvβ6 Reduces Expression of TGFβ in the Col4A3$^{-/-}$ Kidneys

To determine whether decreased kidney fibrosis, detected with 3G9 and 8G6 mAb treatment, was associated with decreased TGF-β expression, kidney sections were immunostained with an anti-TGF-β1 mAb (Figure 10A). The mAb that was used for immunostaining was one that preferentially binds to tissue sections expressing constitutively active TGF-β versus latent TGF-β (data not shown).[24] Treatment of the mice with 3G9 or with 8G6

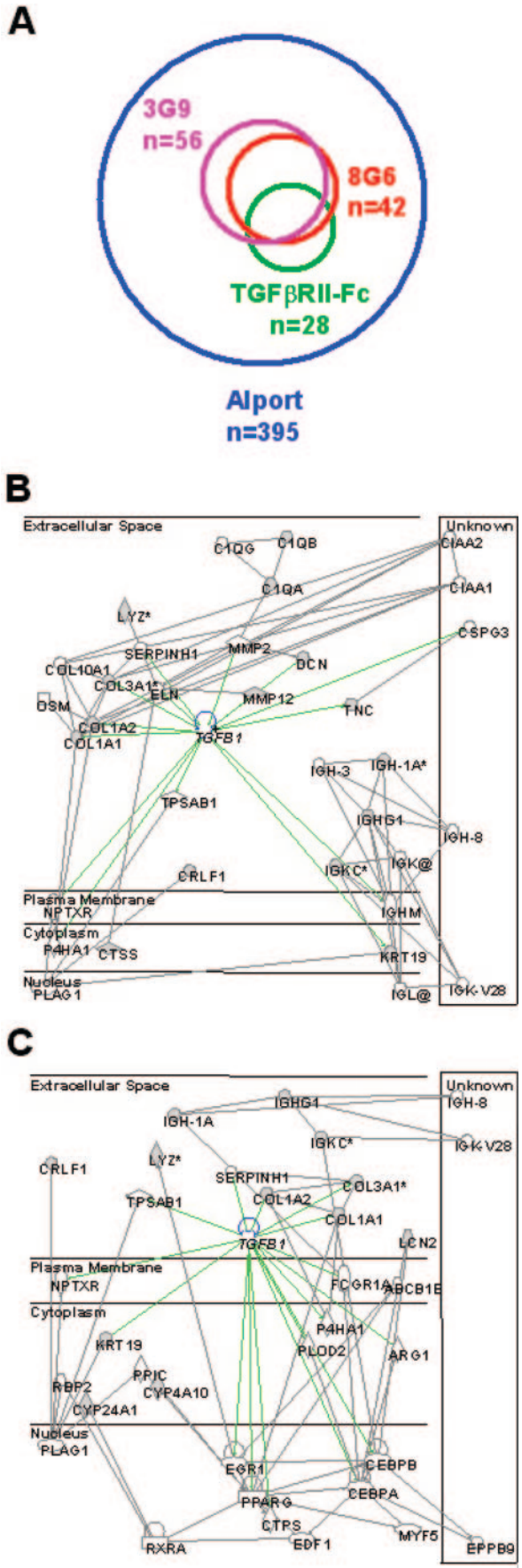

caused a significant reduction in TGF-β1 immunostaining in both the interstitial and glomerular regions of the kidneys. These changes in TGF-β expression were accompanied by analogous changes in the total kidney tissue levels of TGF-β mRNA (Figure 10B). The pattern of TGF-β1 immunostaining indicated that although the expression of $\alpha v\beta 6$ is restricted to the epithelial lining of the kidney tubules, inhibition of $\alpha v\beta 6$ function could lead to decreased TGF-β expression at distal sites such as the glomerular regions, which are not immediately adjacent to areas of $\alpha v\beta 6$ expression. This may suggest that although $\alpha v\beta 6$ could serve as an initial trigger of local TGF-β activation, it could also produce long-range regulatory effects on TGF-β. One possible mechanism of such long-range effects could be based on the ability of TGF-β to activate is own expression in an autocrine or paracrine fashion, leading to the expansion of TGF-β-expressing tissue areas. It also includes the possibility that an initial local inhibition of TGF-β activation by blockade of $\alpha v\beta 6$ interferes with the process of inflammation and fibrosis, which could then indirectly further down modulate TGF-β activity.

Genetic Ablation of the β6 Gene Alleviates Renal Fibrosis in Col4A3$^{-/-}$ Mice

To validate findings from experiments using $\alpha v\beta 6$-blocking mAbs, we generated Col4A3 and $\beta 6$ double knockout mice (Col4A3$^{-/-}$;$\beta 6^{-/-}$). Histological examination of kidneys of age-matched Col4A3$^{-/-}$;$\beta 6^{+/-}$, and Col4A3$^{-/-}$;$\beta 6^{-/-}$ mice confirmed results obtained in studies with $\alpha v\beta 6$-blocking mAbs. There was a significant reduction of SMA immunostaining in kidneys from 7- to 10-week-old Col4A3$^{-/-}$;$\beta 6^{-/-}$ mice compared with age-matched Col4A3$^{-/-}$;$\beta 6^{+/-}$ mice (data not shown). This was accompanied by a dramatic decrease in fibrosis in the glomerular and interstitial regions of the kidneys. This is demonstrated by a reduction of collagen expression and a well-preserved kidney architecture as observed in Trichrome-Masson stained kidneys from 10-week-old Col4A3$^{-/-}$;$\beta 6^{-/-}$ compared with age-matched kidneys from Col4A3$^{-/-}$;$\beta 6^{+/-}$ mice (Figure 11, A and B). Further indication of improved integrity of the kidney structure is shown by an increase in the area of healthy tubules (healthy tubule volume index), by a decrease in the interstitial area (interstitial volume index), and by a reduction in the number of dilated tubules (tubule dilation index) as measured in Trichrome-Masson-stained kidney sections from 10-week-old Col4A3$^{-/-}$;$\beta 6^{-/-}$ mice com-

Figure 9. Subset and network analysis of genes differentially expressed in Col4A3$^{-/-}$ kidneys and modulated by blocking $\alpha v\beta 6$ mAb treatment. **A:** Venn diagram of the probe set lists. The areas of the Venn circles, their unions, and intersections are proportional to the numbers probe sets in the corresponding lists. **B** and **C:** Highest scoring regulatory networks inferred from the lists of probe sets significantly (>2-fold variation between treated and naive Alport kidneys, $P < 0.05$) affected by the $\alpha v\beta 6$-blocking mAbs 3G9 (**B**) and 8G6 (**C**). Edges of the networks show directions of interactions among the genes depicted as the nodes and arranged according to their cellular localization. **Shaded symbols** represent genes affected by the blockade of $\alpha v\beta 6$ function. Their inferred network neighbors are shown as **open symbols**.

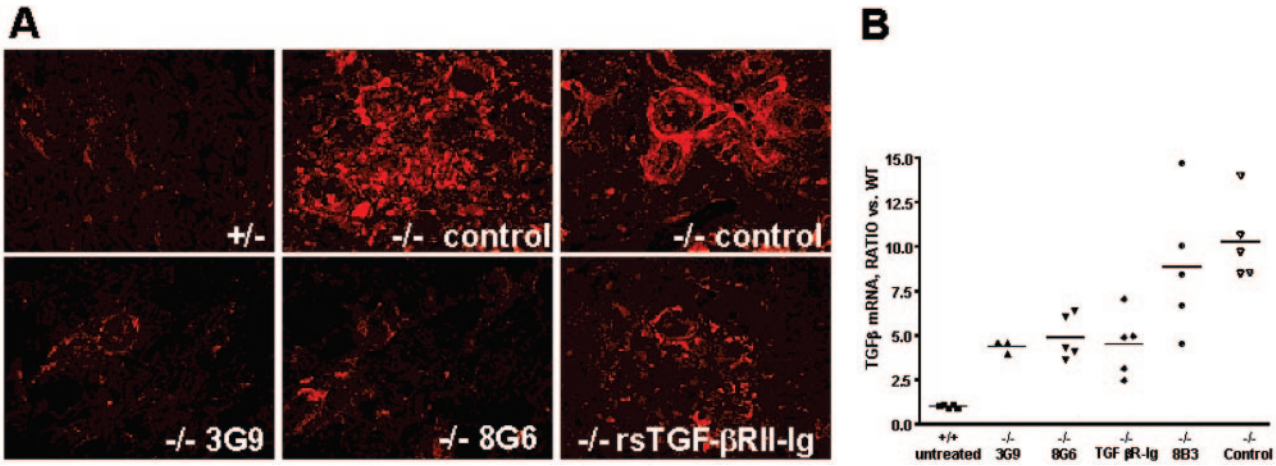

Figure 10. Immunohistochemical and Taqman analysis of TGF-β1 expression. **A:** Kidney sections from Col4A3$^{+/-}$ and Col4A3$^{-/-}$ mice treated with indicated agents were immunostained for TGF-β1 expression. Staining is shown for a representative section from each treatment group. **B:** Taqman analysis of TGF-β1 mRNA levels in various treatment groups.

pared with age-matched Col4A3$^{-/-}$;β6$^{+/-}$ mice (Figure 11C). The consistency of the antifibrotic effects observed with blocking αvβ6 mAb treatment compared with genetic ablation of β6 function indicates that mAb treatment is an efficient approach to blocking αvβ6 function *in vivo*.

Discussion

Progression of renal disease is accompanied by intense tissue remodeling, inflammation, and formation of fibrotic lesions ultimately leading to disruption of the kidney tissue architecture and to loss of renal function. Key molecular mechanisms implicated as major drivers of these events include misregulation of the TGF-β axis accompanied by altered expression of ECM proteins and their receptors in the cells populating fibrotic lesions.[36–38] Elevated expression of TGF-β is a hallmark of fibrotic human tissues,[27–29] and the functional importance of TGF-β in promoting tissue fibrosis has been documented *in vitro* and in animal disease models. Overexpression of TGF-β is sufficient to induce fibroblast activation and angiogenesis *in vivo* and to activate excessive production of ECM in organotypic and cell cultures.[36,39,40] Conversely, genetic or pharmacological disruption of TGF-β signaling provides efficient protection from fibrosis in pulmonary, dermal, and renal fibrosis models.[32,34,35,41–43]

Several studies directed at systemic inhibition of TGF-β function (blocking mAbs, rsTGF-βRII-Ig, and TGF-β receptor kinase inhibitors) have been shown to attenuate fibrosis in animal disease models. However, all of these approaches have been aimed at blocking the activated form of TGF-β, whereas the therapeutic potential of agents that can block TGF-β activation remains less explored. αvβ6 is a TGF-β-inducible integrin expressed at sites of epithelial remodeling and shown to function as a receptor and activator of the latent TGF-β.[11,17,44] The β6 subunit is up-regulated in several forms of renal disease,[10] and its genetic ablation was shown to provide marked protection from injury-induced renal fibrosis in the mouse model of unilateral ureteral obstruction.[45] Similar protection of β6-deficient mice from fibrosis has been observed in the bleomycin lung fibrosis model, suggesting that αvβ6 can mediate fibrosis in diverse tissues.[17,46] Interestingly, unilateral ureteral obstruction-induced phosphorylation of SMAD2, a central mediator of TGF-β signaling was markedly attenuated in the β6-deficient kidneys, indicating that αvβ6 may operate *in vivo* as a part of the TGF-β regulatory circuitry.[45]

Previous studies with β6 knockout mice have provided evidence that αvβ6 can play a role in the initiation of fibrosis, suggesting this integrin as a potential novel therapeutic target. We sought to determine whether pharmacological inhibition of αvβ6 function with blocking mAbs could attenuate renal fibrosis in Col4A3$^{-/-}$ mice, an animal model of the autosomal recessive Alport syndrome.[30,31] Alport syndrome is a hereditary disease caused by mutations in Col4A3, Col4A4, or Col4A5 genes.[47] Defects in these genes result in aberrant assembly of the collagen IV networks and abnormal formation of the glomerular and tubular basement membranes. Alport patients develop progressive glomerulonephritis that leads to end-stage renal disease. We observed up-regulation of αvβ6 in human Alport syndrome and in mouse Col4A3$^{-/-}$ kidney tissues. In Col4A3$^{-/-}$ mouse kidney, the increased expression of αvβ6 was particularly prominent in the tubular epithelium where it preceded and accompanied broad expansion of SMA-positive cells and collagen deposition. Based on this pattern of expression, we hypothesized that αvβ6 becomes up-regulated early in the cycle of epithelial response to injury and may be an important mediator in both the initiation and maintenance of fibrosis in a setting of persistent epithelial damage. The results of our studies show that antibody-mediated blockade of αvβ6 can inhibit initiation and early progression of renal fibrosis and suppress its maintenance. Consistent with previous findings from the β6-deficient mouse model of unilateral ureteral obstruction,[45] the antifibrotic effects of the αvβ6-blocking mAbs observed in our experiments correlated with decreased TGF-β activity and expression. Interestingly, the apparent

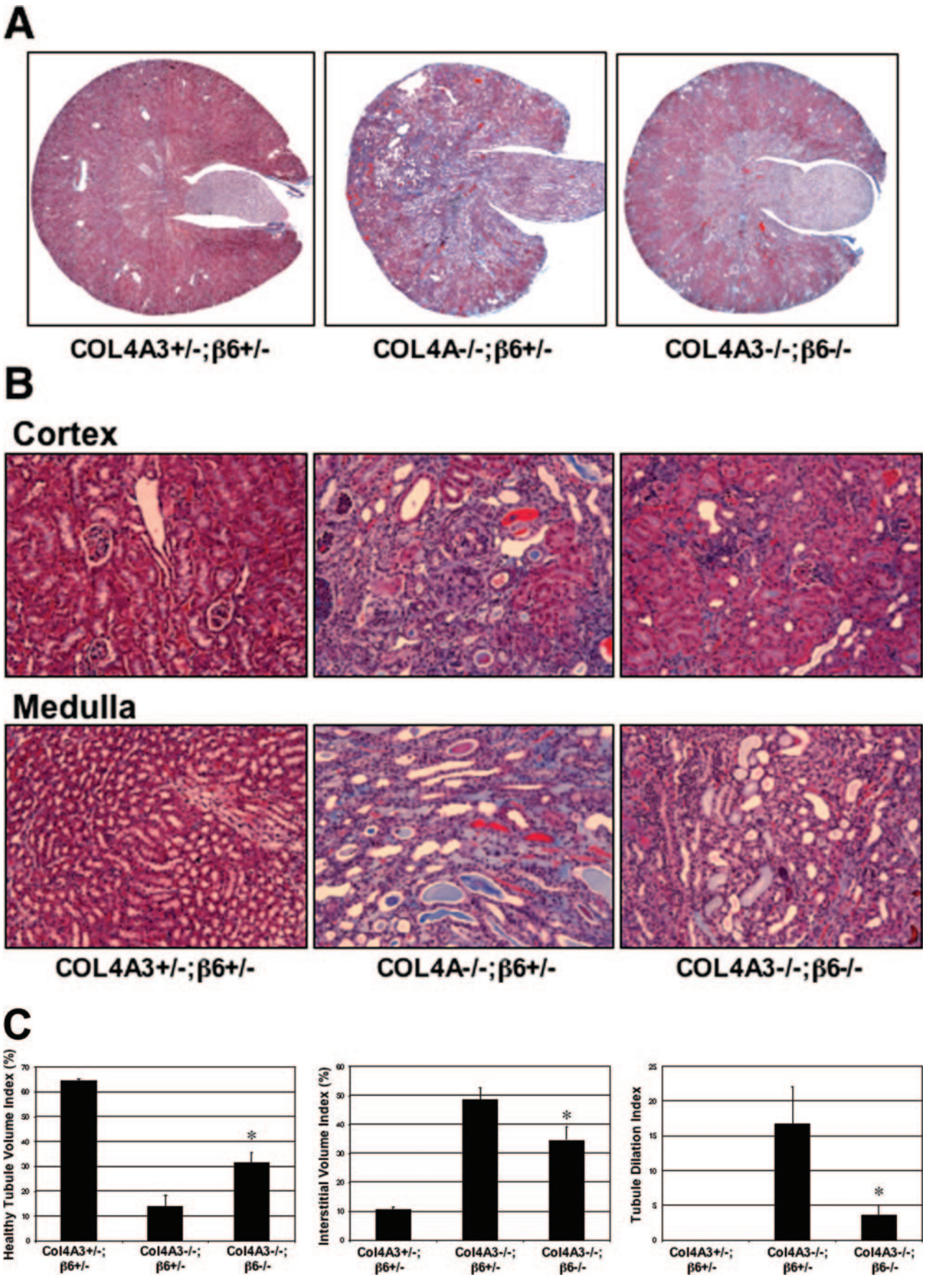
A
COL4A3+/-;β6+/-
COL4A-/-;β6+/-
COL4A3-/-;β6-/-
B
Cortex
Medulla
COL4A3+/-;β6+/-
COL4A-/-;β6+/-
COL4A3-/-;β6-/-
C
Healthy Tubule Volume Index (%)
Interstitial Volume Index (%)
Tubule Dilation Index
Col4A3+/-; β6+/-
Col4A3-/-; β6+/-
Col4A3-/-; β6-/-
*

decrease in TGF-β and SMA expression after αvβ6 mAb treatment occurred not only in the immediate vicinity of αvβ6-positive cells but was detectable in relatively distal tissue regions as well. Although this finding may suggest that αvβ6 can contribute to the activation of the TGF-β axis both directly and in an indirect fashion, eg, via paracrine autoactivation of TGF-β expression, it does not rule out the possibility that αvβ6 blockade may provide protection through extrarenal effects, including altering systemic immune function. We have evaluated serum levels of a number of chemokines and cytokines and peripheral blood populations in mice after 4 weeks of αvβ6 mAb treatment and found no significant changes (data not shown). In addition, only minimal changes in monocytes in the kidneys of Col4A3$^{-/-}$ kidneys was detected by immunohistochemistry with αvβ6 mAb treatment or genetic knockout of the β6 gene (data not shown). Further studies evaluating the functional status of the immune system with αvβ6 mAb treatment or with transplantation studies could address this more completely.

Misregulation and hyperactivity of the TGF-β pathway have been implicated as a prominent mechanism involved in the progression of renal disease in the Col4A3$^{-/-}$ mice.[6] One interesting feature of the TGF-β circuit that could help explain the apparently dominant role of this cytokine in fibrotic disease is the ability of TGF-β to induce its own expression. This raises the possibility that the antifibrotic effects of αvβ6 blockade may be mediated at least in part by indirect mechanisms. This could include downstream effects on TGF-β expression by altering inflammation and fibrosis locally and interfering with subsequent increased TGF-β activity. Because αvβ6 can be induced by TGF-β and promote latent TGF-β activation, we explored the functional relationship between TGF-β and αvβ6 in mediating the Col4A3$^{-/-}$ kidney pathology. We compared the impacts of the αvβ6 mAbs and rsTGF-βRII-Ig on the expression of disease-associated transcripts in the kidneys of Col4A3$^{-/-}$ mice. This comparison has revealed a distinct functional association of the αvβ6-dependent genes with TGF-β and a close similarity of the patterns of gene modulation by the αvβ6 mAbs and by rsTGF-βRII-Ig. Furthermore, treatment of Col4A3$^{-/-}$ mice with αvβ6-blocking mAbs inhibited the kidney expression of TGF-β. These findings show that the disease-modifying effects of the inhibitory αvβ6 mAbs could result from inhibition of TGF-β function, possibly via suppression of αvβ6-mediated activation of the latent TGF-β in the diseased tissue. One intriguing aspect of the above data is the inhibition of pro-inflammatory gene expression through the blockade of αvβ6 or TGF-β. TGF-β has well-established anti-inflammatory and immunosuppressive functions; however, the patterns of gene modulation by rsTGF-βRII-Ig and by the anti-αvβ6 mAbs in our experiments were indicative of a pro-inflammatory function of TGF-β in the Alport disease model. Although the actual mechanism of this apparent pro-inflammatory effect needs further investigation, it could be based on the known ability of TGF-β to induce growth arrest and death of epithelial cells.[33,48–50] Because epithelial damage provides an important mechanism for the activation of early innate immune responses to tissue injury, the apparent pro-inflammatory function of TGF-β suggested by our data could be indirect and mediated by TGF-β-promoted injury to the kidney epithelium. According to this model, αvβ6 may function as an important component of the TGF-β-dependent mechanism of epithelial remodeling, and misregulation of its function in disease could further promote disease-associated tissue damage and inflammation.

It should be noted that although treatment of Col4A3$^{-/-}$ mice with αvβ6 mAbs or rsTGF-βRII-Ig inhibited interstitial and glomerular fibrosis, we observed no significant inhibition of proteinuria and BUN levels with either treatment (data not shown). Similar separation of antifibrotic effects from progressive loss of renal function was previously observed in Alport mice treated with the TGF-β pathway inhibitor, rsTGF-βRII-Ig. In these studies, blockade of the TGF-β pathway inhibited interstitial and glomerular fibrosis but did not improve glomerular function, including proteinuria. The inability to affect kidney function was attributed to the failure to inhibit effacement of the podocyte processes caused by improper composition of the Col4A3-deficient glomerular basement membrane (GBM).[7] Consistent with these findings, we observed podocyte effacement and GBM alterations by transmission electron microscopy in kidneys of the Col4A3$^{-/-}$;β6$^{-/-}$ mice (data not shown). These findings indicate that inhibition of the TGF-β pathway does not alter the structural integrity of the GBM in Alport mice. These results are consistent with the Alport model having aberrant assembly of the ColIV networks and structural abnormalities in the GBM that drives the onset and progression of glomerular and interstitial fibrosis. Other studies in the Alport model have also separated antifibrotic effects from improvement in kidney function.[51,52] Given the growing evidence implicating αvβ6 as a component of the TGF-β axis, the above findings suggest that in renal fibrosis, TGF-β function may be central to regulation of kidney inflammation and fibroblast activation but is not critical for the regulation of podocyte-GBM interactions and GBM remodeling.

The results of our study demonstrate that αvβ6 is highly up-regulated in human kidney disease, and targeting of αvβ6 with function-blocking antibodies may provide an effective novel approach to therapeutic modulation of renal fibrosis. Because the expression of αvβ6 is largely restricted to epithelial cells in the diseased tissue, this approach allows for selective local suppression of TGF-β function. Because TGF-β is expressed in a variety of cells and tissue types, and plays an important role in regulating a number of different homeostatic processes, blocking αvβ6 function offers a potentially safer alterna-

Figure 11. Trichrome staining for collagen expression in kidneys and quantitation of healthy tubule area. Whole kidney sections (**A**) and kidney sections (**B**) shown at ×20 for 10-week-old Col4A3$^{+/-}$;β6$^{+/-}$, Col4A3$^{-/-}$;β6$^{+/-}$, and Col4A3$^{-/-}$;β6$^{-/-}$ mice. Representative sections are shown for cortex and medullary regions of the kidneys. **C:** Quantitation of area of healthy tubules (healthy tubule volume index), area of degenerated tubules and interstitial space (interstitial volume index), and number of dilated tubules (tubular dilation index). *$P < 0.001$ comparing Col4A3$^{-/-}$;β6$^{-/-}$ with Col4A3$^{-/-}$;β6$^{+/-}$ mice.

tive to systemic inhibition of TGF-β in those diseases where the $\alpha v\beta 6$ integrin is up-regulated.

Acknowledgments

We thank Dr. Mary Helen Barcellos-Hoff (Lawrence Berkeley National Laboratory, Berkeley, CA for providing 293 cell xenograft sections to evaluate mAbs for binding to active versus latent TGF-β in immunohistochemistry. Special thanks to Sarah Ryan (Biogen Idec) for providing advice for carrying out studies in Col4A3$^{-/-}$ mice.

References

1. Okada H, Kalluri R: Cellular and molecular pathways that lead to progression and regression of renal fibrogenesis. Curr Mol Med 2005, 5:467–474
2. Sheppard D: Functions of pulmonary epithelial integrins: from development to disease. Physiol Rev 2003, 83:673–686
3. Norman JT, Fine LG: Progressive renal disease: fibroblasts, extracellular matrix, and integrins. Exp Nephrol 1999, 7:167–177
4. Border WA, Noble NA: Interactions of transforming growth factor-beta and angiotensin II in renal fibrosis. Hypertension 1998, 31:181–188
5. Wang W, Koka V, Lan HY: Transforming growth factor-beta and Smad signalling in kidney diseases. Nephrology 2005, 10:48–56
6. Sampson NS, Ryan ST, Enke DA, Cosgrove D, Koteliansky V, Gotwals P: Global gene expression analysis reveals a role for the alpha 1 integrin in renal pathogenesis. J Biol Chem 2001, 276:34182–34188
7. Cosgrove D, Rodgers K, Meehan D, Miller C, Bovard K, Gilroy A, Gardner H, Kotelianski V, Gotwals P, Amattucci A, Kalluri R: Integrin $\alpha 1\beta 1$ and transforming growth factor-$\beta 1$ play distinct roles in Alport glomerular pathogenesis and serve as dual targets for metabolic therapy. Am J Pathol 2000, 157:1649–1659
8. Hamerski DA, Santoro SA: Integrins and the kidney: biology and pathobiology. Curr Opin Nephrol Hypertens 1999, 8:9–14
9. Zambruno G, Marchisio PC, Marconi A, Vaschieri C, Melchiori A, Giannetti A, De Luca M: Transforming growth factor-$\beta 1$ modulates $\beta 1$ and $\beta 5$ integrin receptors and induces the de novo expression of the $\alpha v\beta 6$ heterodimer in normal human keratinocytes: implications for wound healing. J Cell Biol 1995, 129:853–865
10. Trevillian P, Paul H, Millar E, Hibberd A, Agrez MV: Alpha(v)beta(6) integrin expression in diseased and transplanted kidneys. Kidney Int 2004, 66:1423–1433
11. Breuss JM, Gallo J, DeLisser HM, Klimanskaya IV, Folkesson HG, Pittet JF, Nishimura S, Aldape K, Landers DV, Carpenter W, Gillett N, Sheppard D, Matthay MA, Albelda SM, Kramer RH, Pytella R: Expression of the $\beta 6$ subunit in development, neoplasia and tissue repair suggests a role in epithelial remodeling. J Cell Sci 1995, 108:2241–2251
12. Breuss JM, Gillett N, Lu L, Sheppard D, Pytella R: Restricted distribution of integrin $\beta 6$ mRNA in primate epithelial tissues. J Histochem Cytochem 1993, 41:1521–1527
13. Häkkinen L, Hildebrand HC, Berndt A, Kosmehl H, Larjava H: Immunolocalization of tenascin-C, $\alpha 9$ integrin subunit, and $\alpha v\beta 6$ integrin during wound healing in human oral mucosa. J Histochem Cytochem 2000, 48:985–998
14. Arend LJ, Smart AM, Briggs JP: Mouse $\beta 6$ integrin sequence, pattern of expression, and role in kidney development. J Am Soc Nephrol 2000, 11:2297–2305
15. Häkkinen L, Koivisto L, Gardner H, Saarialho-Kere U, Carroll JM, Lakso M, Rauvala H, Laato M, Heino J, Larjava H: Increased expression of $\beta 6$-integrin in skin leads to spontaneous development of chronic wounds. Am J Pathol 2004, 164:229–242
16. Huang XZ, Wu J, Spong S, Sheppard D: The integrin $\alpha v\beta 6$ is critical for keratinocyte migration on both its known ligand, fibronectin, and on vitronectin. J Cell Sci 1998, 111:2189–2195
17. Munger JS, Huang X, Kawakatsu H, Griffiths MJD, Dalton SL, Wu J, Pittet JF, Kaminski N, Garat C, Matthay MA, Rifkin DB, Sheppard D: The integrin $\alpha v\beta 6$ binds and activates latent TGF$\beta 1$: a mechanism for regulating pulmonary inflammation and fibrosis. Cell 1999, 96:319–328
18. Yokosaki Y, Monis H, Chen A, Sheppard D: Differential effects of the integrins alpha9beta1, alphavbeta3, and alphavbeta6 on cell proliferative responses to tenascin: roles of the beta subunit extracellular and cytoplasmic domains. J Biol Chem 1996, 271:24144–24150
19. Annes JP, Rifkin DB, Munger JS: The integrin $\alpha v\beta 6$ binds and activates latent TGF$\beta 3$. FEBS Lett 2002, 511:65–68
20. Munger JS, Harpel JG, Gleizes PE, Mazzieri R, Nunes I, Rifkin DB: Latent transforming growth factor-β: structural feature and mechanisms of activation. Kidney Int 1997, 51:1376–1382
21. Khalil N: TGF-beta: from latent to active. Microbes Infect 1999, 1:1255–1263
22. Barcellos-Hoff MH: Latency and activation in the control of TGF-β. J Mammary Gland Biol Neoplasia 1996, 1:353–363
23. Weinreb PH, Simon KJ, Rayhorn P, Yang WJ, Leone DR, Dolinski BM, Pearse BR, Yokota Y, Kawakatsu H, Atakilit A, Sheppard D, Violette SM: Function-blocking integrin alphavbeta6 monoclonal antibodies. J Biol Chem 2004, 279:17875–17887
24. Barcellos-Hoff MH, Ehrhart EJ, Kalia M, Jirtle R, Flanders KC, Tsang ML-S: Immunohistochemical detection of active transforming growth factor-β in situ using engineered tissue. Am J Pathol 1995, 147:1228–1237
25. Vielhauer V, Anders HJ, Mack M, Cihak J, Strutz F, Stangassinger M, Luckow B, Grone H-J, Schlondorff D: Obstructive nephropathy in the mouse: progressive fibrosis correlates with tubulointerstitial chemokine expression and accumulation of CC chemokine receptor 2- and 5-positive leukocytes. J Am Soc Nephrol 2001, 12:1173–1187
26. Anders HJ, Vielhauer V, Frink M, Linde Y, Cohen CD, Blattner SM, Kretzler M, Strutz F, Mack M, Grone H-J, Onuffer J, Horuk R, Nelson PJ, Schlondorff D: A chemokine receptor CCR-1 antagonist reduces renal fibrosis after unilateral ureter ligation. J Clin Invest 2002, 109:251–259
27. Yamamoto T, Nakamura T, Noble NA, Ruoslahti E, Border WA: Expression of transforming growth factor beta is elevated in human and experimental diabetic nephropathy. Proc Natl Acad Sci USA 1993, 90:1814–1818
28. Yamamoto T, Noble NA, Cohen AH, Nast CC, Hishida A, Gold LI, Border WA: Expression of transforming growth factor-beta isoforms in human glomerular diseases. Kidney Int 1996, 49:461–469
29. Shihab FS, Yamamoto T, Nast CC, Cohen AH, Noble NA, Gold LI, Border WA: Transforming growth factor-beta and matrix protein expression in acute and chronic rejection of human renal allografts. J Am Soc Nephrol 1995, 6:286–294
30. Cosgrove D, Meehan D, Grunkemeyer JA, Kornak JM, Sayers R, Hunter WJ, Samuelson GC: Collagen COL4A3 knockout: a mouse model for autosomal Alport syndrome. Genes Dev 1996, 10:2981–2992
31. Miner JH, Sanes JR: Molecular and functional defects in kidneys of mice lacking collagen $\alpha 3$(IV): implications for Alport syndrome. J Cell Biol 1996, 135:1403–1413
32. Sharma K, Jin Y, Guo J, Ziyadeh FN: Neutralization of TGF-beta by an anti-TGF-beta antibody attenuates kidney hypertrophy and the enhanced extracellular matrix gene expression in STZ-induced diabetic mice. Diabetes 1996, 45:522–530
33. Miyajima A, Chen J, Lawrence C, Ledbetter S, Soslow RA, Stern J, Jha S, Pigato J, Lemer ML, Poppas DP, Vaughan ED, Felsen D: Antibody to transforming growth factor-β ameliorates tubular apoptosis in unilateral ureteral obstruction. Kidney Int 2000, 58:2310–2313
34. Ziyadeh FN, Hoffman BB, Han DC, Iglesias-de la Cruz MC, Hong SW, Isono M, Chen S, McGowan TA, Sharma K: Long-term prevention of renal insufficiency, excess matrix gene expression, and glomerular mesangial matrix expansion by treatment with monoclonal antitransforming growth factor-β antibody in *db/db* diabetic mice. Proc Natl Acad Sci USA 2000, 97:8015–8020
35. Kasuga H, Ito Y, Sakamoto S, Kawachi H, Shimizu F, Yuzawa Y, Matsuo S: Effects of anti-TGF-β type II receptor antibody on experimental glomerulonephritis. Kidney Int 2001, 60:1745–1755
36. Roberts AB, Sporn MB: Regulation of endothelial cell growth, architecture, and matrix synthesis by TGF-beta. Am Rev Respir Dis 1989, 140:1126–1128
37. Eickelberg O, Kohler E, Reichenberger F, Bertschin S, Woodtli T, Erne P, Perruchoud AP, Roth M: Extracellular matrix deposition by primary

human lung fibroblasts in response to TGF-beta1 and TGF-beta3. Am J Physiol 1999, 276:L814–L824
38. Varga J, Rosenbloom J, Jimenez SA: Transforming growth factor beta (TGF beta) causes a persistent increase in steady-state amounts of type I and type III collagen and fibronectin mRNAs in normal human dermal fibroblasts. Biochem J 1987, 247:597–604
39. König A, Bruckner-Tuderman L: Transforming growth factor-beta promotes deposition of collagen VII in a modified organotypic skin model. Lab Invest 1994, 70:203–209
40. Sime PJ, Xing Z, Graham FL, Csaky KG, Gauldie J: Adenovector-mediated gene transfer of active transforming growth factor-β1 induces prolonged severe fibrosis in rat lung. J Clin Invest 1997, 100:768–776
41. Laping NJ: ALK5 inhibition in renal disease. Curr Opin Pharmacol 2003, 3:204–208
42. Bonniaud P, Kolb M, Galt T, Robertson J, Robbins C, Stampfli M, Lavery C, Margetts PJ, Roberts AB, Gauldie J: Smad3 null mice develop airspace enlargement and are resistant to TGF-beta-mediated pulmonary fibrosis. J Immunol 2004, 173:2099–2108
43. Inazaki K, Kanamaru Y, Kojima Y, Sueyoshi N, Okumura K, Kaneko K, Yamashiro Y, Ogawa H, Nakao A: Smad3 deficiency attenuates renal fibrosis, inflammation, and apoptosis after unilateral ureteral obstruction. Kidney Int 2004, 66:597–604
44. Sheppard D: Integrin-mediated activation of transforming growth factor-{beta}1 in pulmonary fibrosis. Chest 2001, 120:49S–53S
45. Ma LJ, Yang H, Gaspert A, Carlesso G, Barty MM, Davidson JM, Sheppard D, Fogo AB: Transforming growth factor-β-dependent and independent pathways of induction of tubulointerstitial fibrosis in β6−/− mice. Am J Pathol 2003, 163:1261–1273
46. Kaminski N, Allard JD, Pittet JF, Fengrong Z, Griffiths MJD, Morris D, Huang X, Sheppard D, Heller RA: Global analysis of gene expression in pulmonary fibrosis reveals distinct programs regulating lung inflammation and fibrosis. Proc Natl Acad Sci USA 2000, 97:1778–1783
47. Torra R, Tazon-Vega B, Ars E, Ballarin J: Collagen type IV ({alpha}3-{alpha}4) nephropathy: from isolated haematuria to renal failure. Nephrol Dial Transplant 2004, 19:2429–2432
48. Böttinger EP, Bitzer M: TGF-beta signaling in renal disease. J Am Soc Nephrol 2002, 13:2600–2610
49. Goumenos DS, Tsamandas AC, El Nahas AM, Thomas G, Tsakas S, Sotsiou F, Bonikos DS, Vlachojannis JG: Apoptosis and myofibroblast expression in human glomerular disease: a possible link with transforming growth factor-beta-1. Nephron 2002, 92:287–296
50. Dai C, Yang J, Liu Y: Transforming growth factor-beta1 potentiates renal tubular epithelial cell death by a mechanism independent of Smad signaling. J Biol Chem 2003, 278:12537–12545
51. Chen D, Jefferson B, Harvey SJ, Zheng K, Gartley CJ, Jacobs RM, Thorner PS: Cyclosporine A slows the progressive renal disease of Alport syndrome (X-linked hereditary nephritis): results from a canine model. J Am Soc Nephrol 2003, 14:690–698
52. Ninichuk V, Gross O, Segerer S Hoffman R, Radomska E, Buchstaller A, Huss R, Akis N, Schlondorff D, Anders HJ: Multipotent mesenchymal stem cells reduce interstitial fibrosis but do not delay progression of chronic kidney disease in collagen4A3-deficient mice. Kidney Int 2006, 70:121–129